Aalborg Universitet

AALBORG UNIVERSITY

The inflammatory response of the supraspinatus muscle in rotator cuff tear conditions

Frich, Lars Henrik; Fernandes, Livia Rosa; Schrøder, Henrik Daa; Hejbøl, Eva Kildall; Nielsen, Pernille Vinther; Jørgensen, Puk Hvirgel; Stensballe, Allan; Lambertsen, Kate Lykke

ONLINE ARTICLES

The inflammatory response of the supraspinatus muscle in rotator cuff tear conditions

Lars Henrik Frich, MD, PhD[a,b,c,*], Livia Rosa Fernandes, PhD[d],
Henrik Daa Schrøder, DMSc[e], Eva Kildall Hejbøl, PhD[e],
Pernille Vinther Nielsen, BSc[b], Puk Hvirgel Jørgensen, MSc[f], Allan Stensballe, PhD[f],
Kate Lykke Lambertsen, PhD[d,g,h]

[a]Department of Orthopaedics, Odense University Hospital, Odense, Denmark
[b]The Orthopaedic Research Unit, University of Southern Denmark, Odense, Denmark
[c]Institute of Molecular Medicine, University of Southern Denmark, Odense, Denmark
[d]Department of Neurobiology Research, Institute of Molecular Medicine, University of Southern Denmark, Odense, Denmark
[e]Department of Pathology, Odense University Hospital, Odense, Denmark
[f]Department of Health Science and Technology, Aalborg University, Aalborg, Denmark
[g]Department of Neurology, Odense University Hospital, Odense, Denmark
[h]BRIDGE (Brain Research – Inter-Disciplinary Guided Excellence), University of Southern Denmark, Odense, Denmark

Background: Rotator cuff (RC) disorders involve a spectrum of shoulder conditions from early tendinopathy to full-thickness tears leading to impaired shoulder function and pain. The pathology of RC disorder is, nonetheless, still largely unknown. Our hypothesis is that a supraspinatus (SS) tendon tear leads to sustained inflammatory changes of the SS muscle along with fatty infiltration and muscle degeneration, which are threshold markers for poor RC muscle function. The aim of this study was to determine the extent of this muscle inflammation in conjunction with lipid accumulation and fibrosis in RC tear conditions.
Methods: We used proteomics, histology, electrochemiluminescence immunoassay, and quantitative polymerase chain reaction analyses to evaluate inflammatory and degenerative markers and fatty infiltration in biopsies from 22 patients undergoing surgery with repair of a full-thickness SS tendon tear.
Results: Bioinformatic analysis showed that proteins involved in innate immunity, extracellular matrix organization, and lipid metabolism were among the most upregulated, whereas mitochondrial electronic transport chain along with muscle fiber function was among the most downregulated. Histologic analysis confirmed changes in muscle fiber organization and the presence of inflammation and fatty infiltration. Inflammation appeared to be driven by a high number of infiltrating macrophages, accompanied by elevated matrix metalloprotease levels and changes in transforming growth factor-β and cytokine levels in the SS compared with the deltoid muscle.
Conclusions: We demonstrated massive SS muscle inflammation after the tendon tear combined with fatty infiltration and degeneration. The regulation of tissue repair is thus extremely complex, and it may have opposite effects at different time points of healing. Inhibition or stimulation of muscle inflammation may be a potential target to enhance the outcome of the repaired torn RC.

*Reprint requests: Lars Henrik Frich, MD, PhD, Department of Orthopaedics, Odense University Hospital, J.B. Winsloewsvej 4, DK-5000 Odense C, Denmark.
E-mail address: lars.henrik.frich@rsyd.dk (L.H. Frich).

Rotator cuff (RC) lesions are some of the most common shoulder conditions in humans and can lead to weakness, pain, and limited/reduced mobility. The prevalence of RC tears is age-dependent, and both partial- and full-thickness RC tears increase markedly after 50 years of age.[48] The etiology of RC diseases is multifactorial with frequent involvement of the supraspinatus (SS) tendon.[5] Full-thickness SS tears do not heal spontaneously, and surgically repaired RC tears tend to heal poorly.[14,32] A recent Cochrane review questioned whether repair of RC tears provides meaningful benefit to patients with symptomatic RC tears.[23] There is, therefore, a pressing need to better understand the pathophysiology behind RC tear conditions in order to improve results after surgical repair of RC tendon tears.

In full-thickness RC tears, increased numbers of immune cells have been demonstrated in the synovial tissue adjacent to the SS tendon[1] and an increase in tear size correlated with a greater proinflammatory response in the synovium.[6,44] Recent data suggest that the RC muscles also become inflamed in the presence of an RC tear,[13] and results from experimental models suggest that acute inflammation plays a detrimental role in the onset of chronic muscle damage after RC tears.[16,28] It is also generally agreed that a chronic RC tendon lesion leads to degenerative muscle changes in the form of fatty infiltration and fibrosis.[10]

Several animal studies have provided evidence of significant increases in inflammatory cytokines, growth factors, and matrix metalloproteases (MMPs), indicating muscle inflammation after the experimental RC tendon tear.[16,28] Changes in the biology of human RC muscles in tear conditions remain poorly defined at the cellular level, however, and an RC muscle as a target for inflammation after an RC tear is only sparsely understood.[13,22]

The aim of this study was to provide a more robust understanding of the inflammatory environment of a human SS muscle in RC tear conditions. Our hypothesis is that inflammatory conditions precede disturbances of the muscle architecture and eventually lead to RC muscle fatty infiltration and degeneration. To investigate this, we applied quantitative proteomics followed by histology, multiplex chemiluminescence, and quantitative polymerase chain reaction (qPCR) analyses of inflammation in SS and deltoid muscle biopsies that were harvested from patients undergoing surgery for RC tears.

Materials and methods

Patient cohort

Patients (n = 22) with a relevant shoulder trauma and clinical signs of an RC lesion were recruited (Supplementary Table S1). The median age of lesions was 3.3 months (interquartile range, 2-14 months). Patients underwent preoperative magnetic resonance imaging scan revealing an SS tendon tear, and all tears were confirmed at surgery. Informed written consent was obtained from all patients. The workflow of the project is presented in Figure 1.

Human tissue

The RC and musculotendinous junction of the SS muscle were gently débrided from fascia and bursal tissue using a blunt shaver. SS tendon and muscle biopsies were harvested from the edge of the tendon and approximately 1 cm medial to the tendon, respectively, under direct visualization from the arthroscope. Comparative biopsies were taken from assumed healthy, ipsilateral deltoid muscles. Biopsies were snap-frozen on dry ice and stored at $-80°C$ or fixed in 10% neutral buffered formalin and embedded in paraffin.

Blood samples

Blood samples were obtained in ethylenediamine tetraacetic acid (EDTA)-coated test tubes immediately before surgery to estimate preoperative peripheral inflammation. Hemoglobin, C-reactive protein, and white blood cell counts were analyzed. The patient cohort was also tested for the presence of rheumatic factors (antinuclear, anticyclic citrullinated, and mitochondrial antibodies and rheuma factor).

Histology and immunohistochemistry

SS or deltoid muscle tissue was sectioned into 2-μm-thick sections on a microtome. Immunohistochemistry for CD68 was performed on the OMNIS platform (Dako/Agilent, Glostrup, Denmark) using mouse anti-CD68 (1:50, clone PG-M1) antibody and EnVision FLEX as the detection system, whereas immunohistochemistry for Forkhead box P3 (FOXP3), CD3, and adipophilin was performed on a BenchMark Ultra immunostainer (Ventana Medical Systems, Oro Valley, AZ, USA) using mouse anti-FOXP3 (1:40, clone 236A/E7), rabbit anti-CD3 ("*ready-to-use*," clone 2GV6), and mouse anti-adipophilin (1:50, clone AP125) antibodies and the OptiView-DAB detection system. Parallel sections were stained with hematoxylin and eosin.
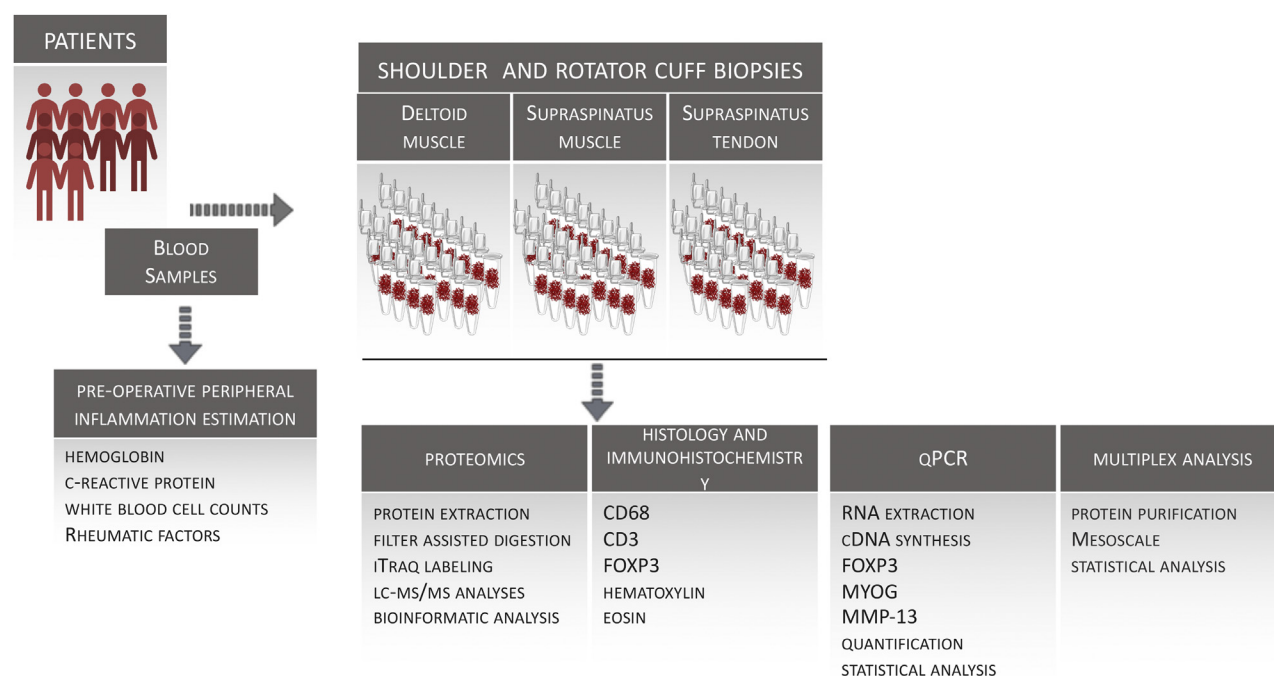
Figure 1 Schematic workflow applied to the study of molecular pathways involved in the RC lesion. Biopsies of the supraspinatus tendon and supraspinatus and deltoid muscle biopsies from 10 patients undergoing surgery for partial- or full-thickness RC were evaluated. *RC*, rotator cuff; *qPCR*, quantitative polymerase chain reaction.

Slides were scanned on a NanoZoomer 2.0 RS scanner (Hamamatsu Photonics, Visiopharm, Hørsholm, Denmark). To produce merged images, NDP view (version 2.6.17; Hamamatsu Photonics) was applied to find identical regions on neighboring cells stained for FOXP3 and CD3, respectively. The images were processed and merged using Photoshop C6 (Adobe Systems, San Jose, CA, USA) and ImageJ/Fiji. The area with muscle tissue in each biopsy was determined using the freehand region function, and the number of CD3 and FOXP3 within this area was manually counted at ×20 magnification.

Proteomics

Homogenization of tissue biopsies

Approximately 1 mm^3 was cut from the frozen tendon and muscle biopsies and was homogenized by bead beating using 0.9-2.0 mm stainless steel beads (Bullet Blender Gold; Next Advance Inc., Troy, NY, USA) in reducing lysis buffer (5% sodium deoxycholate [SDC]; Sigma-Aldrich, St. Louis, MO, USA) and protease inhibitors (cOmplete; Roche, Basel, Swizerland) in 50 mM Trie-thylamonium bicarbonate (TEAB) (Sigma-Aldrich). Protein concentration in lysates was determined by protein A280 and lysates stored at −80°C (DeNoviX, Wilmington, DE, USA).

Samples were further processed using an optimized SDC filter-aided sample preparation protein digestion essentially as[4] using 100 µg of protein starting material in 10 kDa molecular-weight cutoff spin filters (Merch Millipore, Millipore, Singapore). The lysates were reduced (10 mM TCEP) and alkylated (50 mM chloroacetamide) each for 15 minutes in digestion buffer (5% SDC in 50 mM TEAB; Sigma-Aldrich). Overnight trypsin digestion at 37°C was performed by the addition of 200 µL of

0.5% digestion buffer containing trypsin 1:50 (v:v; Pierce, Rockford, IL, USA). Peptides were extracted by acidification and phase separation, where 3:1 (v/v) ethyl acetate of sample volume was added and acidified by adding trifluoroacetic acid (Sigma-Aldrich) to a final concentration of 1% (pH < 2) followed by centrifugation. The collected lower aqueous phase containing the peptides was dried in a vacuum centrifuge and dissolved in 0.1 M TEAB. Peptide concentration in lysates was determined by protein A280 and lysates stored at −80° (DeNoviX).

iTRAQ labeling

A total of 5 µg of each sample was labeled with a 4-plex iTRAQ kit (AB Sciex, Redwood City, CA, USA) according to the manufacturer's instructions. Briefly, samples were redissolved to a total volume of 25 µL of 0.1 M TEAB, pH 8.5, whereafter 290 µL of 96% ethanol was added to iTRAQ reagents. Next, 50 µL of the iTRAQ reagents was transferred to the samples, which were then labeled, mixed after 1 hour of incubation at room temperature, dried, and resuspended in 2% acetonitrile, 0.1% Trifluoroacetic acid (TFA) (Sigma-Aldrich).

iTRAQ sample analysis

Samples were analyzed per UPLC-TandemMS in technical duplicates. Labeled peptides were separated by a nanoUPLC system (Thermo Scientific, Waltham, MA, USA) coupled online to a Q Exactive HF MS (Thermo Scientific) using a reverse phase C18 trapping column setup with a 75 cm main column (Thermo Scientific) with loading in 2% solvent B (0.1% Formic acid (FA) in acetonitrile) gradient and separated by 176-minute gradient from 11%B to 30%B with a constant flow rate at 250 nL/min. MS was operated in positive mode using Top10 data-dependent acquisition

(MS1 m/z 375-1500 at R 120,000) and tandem sequencing using the fixed m/z range at 110 and an MS2 resolution of 15,000.

Database searches

Raw data were processed using Proteome Discoverer v2.3.0.523 (Thermo Scientific). Sequest HT was set as the search engine against the reviewed Uniprot Homo sapiens reference protein database (September 2017). iTRAQ 4-plex labeling of N-terminal and lysine and carbamidomethylation (C) were set as fixed modifications, whereas oxidation (M), deamidation (N/Q), and protein N-terminal acetylation were included as variable modifications. Precursor mass tolerance and fragment mass tolerance were set at 10 ppm and 0.05 Da, respectively. Spectral matches (SPMs) were filtered using a percolator with a strict false discovery rate (FDR) of 1% and a relaxed FDR of 5%. Unique and razor peptides were used for quantification, and iTRAQ channels were normalized to the total peptide amount. Master proteins were filtered for high-protein FDR confidence. MS data have been deposited to the ProteomeXchange Consortium via the PRIDE[38] partner repository with the dataset identifier PXD014037.

Bioinformatic analyses and functional annotation of regulated proteins

Normalized abundances were used for further analyses of proteins identified with 2 or more unique peptides. Data distribution was assessed with Perseus v.1.5.3.2 software, and differentially regulated features were selected using the t-test with a post hoc background-based adjusted P value of $<.05$.[34] Venny 2.1 (http://bioinfogp.cnb.csic.es/tools/venny) was used to compare the regulated proteins among the different comparisons. ToppGene Suite[8] was used for functional enrichment of regulated proteins according to Gene Ontology (GO) terms and pathway analysis. Enriched lists were further accessed by String app on Cytoscape v3.6.1.[43]

Reverse transcription quantitative PCR (RT-qPCR) analysis of *FOXP3*, *MYOG*, and *MMP13* in SS and deltoid muscle tissue

RNA extraction

Muscle biopsies (n = 18/group) were isolated using TRIzol Reagent. Phase separation was performed using chloroform, and isopropyl alcohol was used to precipitate RNA. The RNA concentrations and purities were determined using a Nanodrop Spectrophotometer (Thermo Scientific).

cDNA synthesis

RNA samples were diluted to obtain a concentration of 250 ng/µL, and reverse transcription was performed using an Applied Biosystem kit according to the manufacturer's instructions. The synthesis was performed using an MJ Research PTC-225 Gradient Thermal Cycler (Marshall Scientific, Hampton, NH, USA). cDNA samples were diluted to lower the concentrations to approximately 50 ng/µL.

RT-qPCR

RT-qPCR was performed using a CFX Connect Real-Time PCR Detection System (Bio-Rad, Copenhagen, Denmark) and analyzed using SYBR green. Samples were run against standard curves generated from serial dilutions from a pool of all samples. Values were normalized to *ACTB* (β-actin) as the reference gene and calibrated to a pool of cDNA obtained from 1 pectoralis and 1 subscapularis muscle biopsy. Triplicates of all samples, standards, and negative controls were conducted. To ensure no sign of primer dimer formation or contamination, a no amplification control, a no template control, and a no reverse transcriptase were included as controls.

RT-qPCR cycling conditions were as follows: 10 minutes at 95°C, followed by 40 cycles of denaturing at 95°C for 15 seconds, 30 seconds at annealing temperature, and extension at 72°C at 30 seconds.

Primer sequences were: *ACTB*, sense 5′-GGCCACGGC TGCTTC-3′ and antisense 5′-GTTGGCGTACAGGTCTTTGC-3′ (T_a 52°C and T_m 84°C); *FOXP3*, sense 5′-CCCGGATG TGAGAAGGTCTT-3′ and antisense 5′-TTCTCCTTCTC CAGCACCAG-3′ (T_a 57°C and T_m 82°C); *MYOG*, sense 5′-GCCCTGATGCTAGGAAGCC-3′ and antisense 5′-CTGAAT-GAGGGCGTCCAGTC-3′ (T_a 70°C and T_m 85°C); and *MMP13*, sense 5′-CGC CAG ACA AAT GTG ACC CT-3′ and anti-sense 5′-CAG GCG CCA GAA GAA TCT GT-3′ (T_a 55°C and T_m 77°C). Primer specificity was ensured by generation and evaluation of melting curves. Primers were purchased from TAG Copenhagen (Copenhagen, Denmark).

Electrochemiluminescence analysis

Protein purification

Tendon and muscle samples were homogenized at 4°C in Mesoscale Lysis buffer containing Phosphatase Inhibitor Cocktail 2 and 3 (Sigma-Aldrich) and Complete Mini EDTA-free Protease Inhibitor (Roche). Protein content was measured by the bicinchoninic acid method using the Thermo Scientific Micro BCA Protein Assay Kit (Pierce Chemical Co, Dallas, TX, USA).[39]

Multiplex analysis

Protein concentrations in tendon and muscle samples were measured using an MSD human U-Plex Biomarker Multip-Plex Kit, a U-PLEX human transforming growth factor-β (TGF-β) Combo Kit, a human MMP 3-Plex Ultra-Sensitive Kit, and human TNF-RI and TNF-RII Ultra-Sensitive Kits (all from Mesoscale Rockville, MD, USA), and using the MSD QuickPlex (SQ120) Plate Reader (Mesoscale) according to the manufacturer's instructions. Intercellular adhesion molecule 1 and vascular cell adhesion protein 1 analyses were performed on SS and deltoid muscle tissue using V-PLEX Vascular Injury Panel 2 (Mesoscale). Samples were run in duplex and diluted 2- or 4-fold in Diluent 41 before measurement. Data were analyzed using MSD Discovery Workbench software. The lower limit of detection was a calculated concentration based on a signal 2.5 standard deviation (SD) above the blank (zero) calibrator, and coefficient of variation values below 25% were accepted.

Statistical analysis

To examine differences in protein expression between SS and deltoid muscle tissue, paired Student's t-test was used. Correlation analyses between cytokine, MMPs, and growth factors vs. age of lesion used Spearman's test. To examine the correlation between the relative

expression of *FOXP3*, *MYOG*, and *MMP13* in SS and deltoid muscles, a paired Wilcoxon test was carried out. The outlier test ROUT was used to identify and remove outliers more than 2 SD from the dataset. All statistical analyses were carried out using GraphPad Prism. *P* values ≤.05 were considered statistically significant. Data are presented as mean ± SD or median (interquartile range: 25, 75).

Results

Mass spectrometry–based proteomics analysis shows protein regulation on an RC lesion

Using quantitative mass spectrometry proteomics, a total of 2463 proteins were identified, of which 1895 had 2 or more unique peptides (Supplementary Table S2). Moreover, 417 quantified proteins were shared by all tissues of all patients and could be assessed by principal component analysis (Supplementary Fig. S1, *A*), which showed a clear distribution pattern even in the absence of well-delimited clusters.

To better understand protein regulation underlying RC pathology, the SS muscle protein expression pattern was compared with deltoid as a non-RC shoulder muscle control. A total of 239 proteins were regulated. Of these, 114 were more highly expressed in the SS muscle (Fig. 2, *A*; Supplementary Table S3). GO analysis showed "extracellular matrix organization" and "neutrophil degranulation" among the most enriched biological processes (Supplementary Fig. S2 and Supplementary Table S4), whereas "degradation of extracellular matrix," "innate immune system," and "neutrophil degranulation" were among the enriched pathways of upregulated proteins (Fig. 2, *B*; Supplementary Fig. S2 and Supplementary Table S4). Interestingly, "mitochondrial cellular localization" and "muscle system process" were among the enriched annotations of downregulated proteins (Fig. 2, *B*; Supplementary Fig. S3 and Supplementary Table S4). A detailed list of regulated proteins involved in the abovementioned processes, along with experimental ratio, is provided in Figure 2, *C-K*.

To address the molecular response of different RC tissues, the comparison between the SS muscle and SS tendon showed 139 differentially expressed proteins (Supplementary Table S5). Pathways or gene ontologies related to immune response or inflammatory processes were not enriched among these regulated proteins.

In contrast, pointing toward a common molecular signature between the SS muscle and SS tendon in RC disease, 38 proteins were regulated in both tissues when compared with the deltoid muscle (Supplementary Fig. S1, *B*, and Supplementary Tables S6 and S7). Several of these proteins were related to catalytic activity, with the mitochondrial protein complex being the main cellular component (Supplementary Fig. S1, *C*).

RC lesion results in atrophy and lipid accumulation

Staining with hematoxylin and eosin revealed muscle fiber changes already 1½ months after the tendon lesion represented by internalization of nuclei and muscle fibers of varying size after the tendon tear (Fig. 3, *A*). In addition, pathologic infiltrating adipocytes were detected, as substantial fat infiltration was seen together with arrays of intracellular myonuclei and varying fiber size, suggestive of degeneration (Fig. 3, *B* and *C*).

Inflammatory changes appeared to be intensified from 1½ to 6 months with abundant stromal inflammatory phagocytic cells represented by the presence of CD68$^+$ macrophages (Fig. 3, *D* and *E*). At 24 months, degeneration was clearly seen with a substantial proportion of muscle cells replaced by fat cells indicative of muscle cell degeneration (Fig. 3, *F*). At 24 months, absent or few CD68$^+$ positive cells indicated decreased inflammation. The deltoid muscle did not demonstrate similar inflammatory and degenerative changes (Fig. 3, *G-L*).

Adipophilin/perilipin-2 immunohistochemistry for detection of lipids in myofibers demonstrated that adipophilin was localized to the surface of intracellular lipid droplets (Fig. 4). The expression varied both between patients (please compare Fig. 4, *A*, with Fig. 4, *C*) and between muscles from the same patient (please compare Fig. 4, *A*, with Fig. 4, *B*). Regional differences within muscles were also seen (Fig. 4), and some individual fibers presented increased lipid accumulation both as number and size of droplets (arrows in in Fig. 4 *A*, *C*, *D*).

RC tendon tear leads to changes in inflammatory mediators in the SS muscle

None of the patients showed any signs of peripheral inflammation as mean blood leukocyte counts, hemoglobin, and C-reactive protein values were within normal ranges and all patients were negative for rheumatic factors. Given the findings of significant changes in the proteome of the SS compared with the deltoid muscle after the RC tear, we investigated changes in a variety of pro- and anti-inflammatory cytokines, chemokines, receptors, and growth factors (Fig. 5 and Table I). We found lower CCL19 levels (Fig. 5, *A*) but higher CXCL5 levels (Fig. 5, *B*) in the SS compared with the deltoid muscle. IL-1β (Fig. 5, *C*), IL-6 (Fig. 5, *D*), IL-8 (Fig. 5, *E*), and IL-33 levels (Fig. 5, *F*) were higher in the SS compared with the deltoid muscle. IL-7 (Fig. 5, *G*), IL-15 (Fig. 5, *H*), IL-17A (Fig. 5, *I*), and IFN-α2a levels (Fig. 5, *J*) were lower in the SS compared with the deltoid muscle. Despite comparable levels of TNF (Fig. 5, *K*), TNFR1 (Fig. 5, *L*) and TNFR2 (Fig. 5, *M*) levels were changed in the SS muscle compared with the deltoid after the RC tendon tear. G-CSF levels were lower in the SS muscle compared with the deltoid (Fig. 5, *N*).
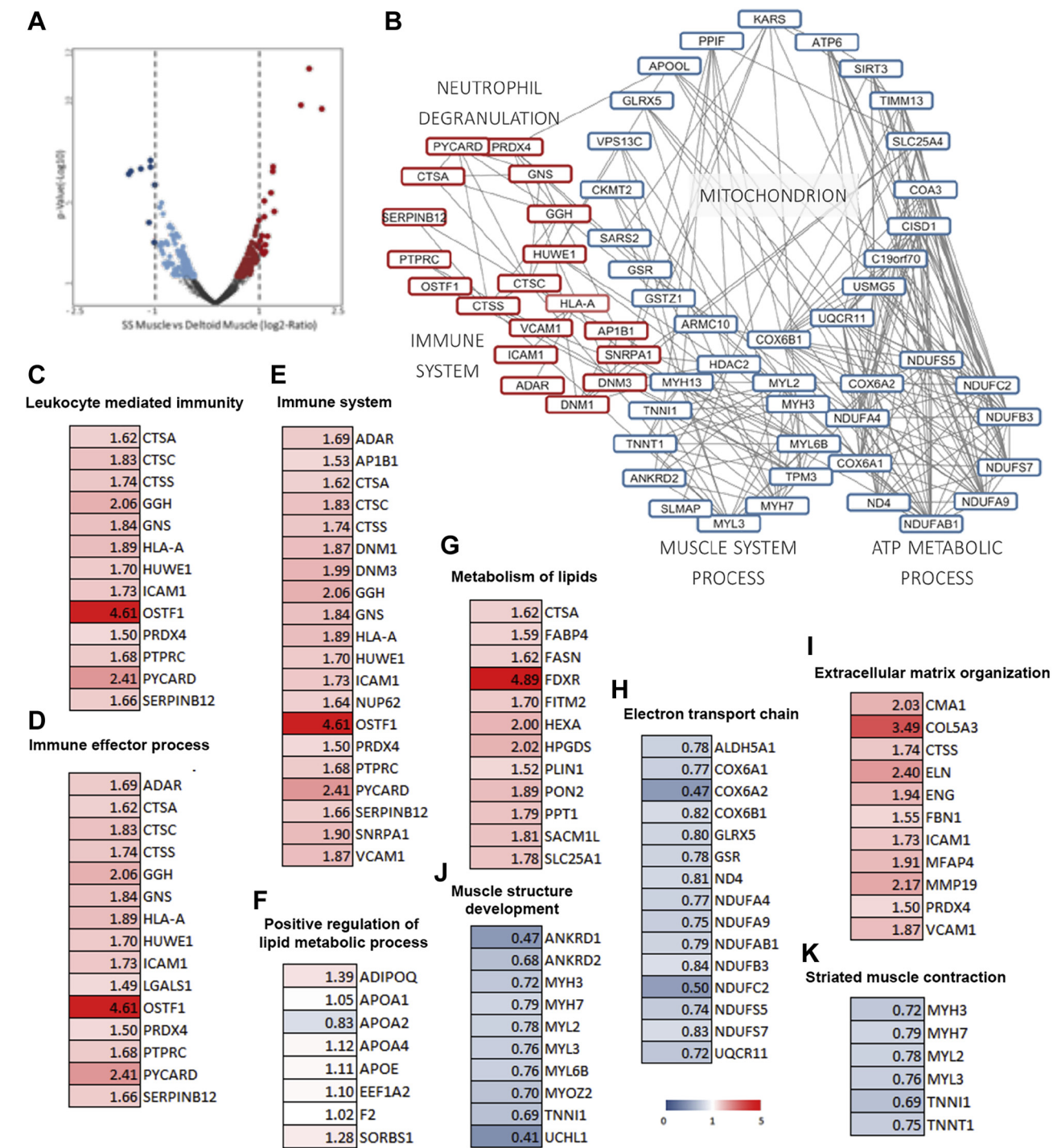
Figure 2 Proteomics of muscle biopsies. (**A**) Differentially regulated protein pattern between the SS and deltoid muscles from patients with the RC lesion (FDR 5%). Downregulated proteins are represented in blue and upregulated in red. Dotted lines highlight proteins at least 2 times over-represented in each tissue. (**B**) Protein-protein network of SS vs. deltoid muscle–regulated proteins grouped according to functional enrichment. Underrepresented proteins in the SS muscle are shown in blue, whereas over-represented are shown in red. (**C-K**) Levels of upregulated (red) or downregulated (blue) proteins involved in (**C**) leukocyte-mediated immunity, (**D**) immune effector process, (**E**) immune system, (**F**) positive regulation of lipid metabolic processes, (**G**) metabolism of lipids, (**H**) electron transport chain, (**J**) muscle structure development, (**I**) extracellular matrix organization, and (**K**) striated muscle contraction as measured by proteomics (n = 10 muscles per group). *ADAR*, double-stranded RNA-specific adenosine deaminase; *ADIPOQ*, adiponectin; *ALDH5A1*, succinate-semialdehyde dehydrogenase, mitochondrial; *ANKRD1*, ankyrin repeat domain-containing protein 1; *ANKRD2*, ankyrin repeat domain-containing protein 2; *AP1B1*, AP-complex subunit beta-1; *APOA1*, apolipoprotein A-1; *APOA2*, apolipoprotein A-2; *APOA4*, apolipoprotein A-4; *APOE*, apolipoprotein E; *CMA1*, chymase; *COL5A3*, collagen alpha-3(V) chain; *COX6A1*, cytochrome c oxidase

We observed no significant correlation between age of lesion and CCL19 ($r = -0.05$, $P = 1$), CXCL5 ($r = -0.26$, $P = .31$), IL-1β ($r = -0.30$, $P = .3$), IL-6 ($r = -0.48$, $P = .07$), IL-8 ($r = -0.43$, $P = .11$), IL-33 ($r = 0.16$, $P = .54$), IL-7 ($r = 0.35$, $P = .39$), IL-15 ($r = 0.07$, $P = .79$), IL-17A ($r = 0.09$, $P = .76$), IFN-α2a ($r = 0.39$, $P = .3$), TNF ($r = -0.39$, $P = .15$), TNFR1 ($r = -0.4$, $P = .29$), TNFR2 ($r = -0.16$, $P = .66$), or G-CSF ($r = 0.16$, $P = .71$).

Finally, several cytokine levels were similar in the SS and deltoid muscle (Table I). The concentration of most cytokines, chemokines, growth factors, and MMPs was high in the SS tendon (Supplementary Table S8).

The regenerative potential appears to be impaired in the SS muscle after the RC tendon tear

IL-17 production characterizes proinflammatory T-helper 17 lymphocytes (Th17) and innate immune cells.[11] Th17 has been shown to have opposing effects in the immune response from regulatory T cells (Tregs),[49] which is important in muscle regeneration (reviewed in the paper by Burzyn et al[7]) and whose master gene is the transcription factor FOXP3. We found decreased IL-17A levels in the SS muscle compared with the deltoid muscle (Fig. 5, G). Therefore, we next investigated FOXP3 mRNA expression and found that FOXP3 mRNA levels were significantly lower in the SS muscle compared with the deltoid muscle (Fig. 6, A). However, when we counted FOXP3+ cells (Fig. 6, B) and CD3+ T cells (Fig. 6, C) in SS and deltoid muscle tissue sections (Fig. 6, D), we did not observe any significant differences in the number of FOXP3+ cells/mm² or CD3+ T cells/mm². Approximately 7.5% of all T cells in the SS muscle were FOXP3+ Tregs (overlay in Fig. 6, D, upper panel), and approximately 13% of all T cells in the deltoid muscle were FOXP3+ Tregs (overlay in Fig. 6, D, middle panel). The number of T cells/mm² was, however, quite variable (Fig. 6, D).

To investigate gene expression levels involved in myogenesis, we estimated MYOG expression and found the relative mRNA levels to be significantly decreased in the SS compared with the deltoid muscle (Fig. 6, E).

Changes in MMPs and TGFs after the RC tendon tear

As GO analysis showed changes in proteins involved in "extracellular matrix organization," we investigated changes in the levels of 4 MMPs known to be involved in the degradation of the extracellular matrix.[37]

We did not observe any differences in MMP1 levels between the SS and deltoid muscle (Fig. 7, A). However, levels of MMP3 (that is known to degrade collagen types II-IV, IX, and X and to have important regulatory functions such as activation of other MMPs) were significantly higher in the SS compared with the deltoid muscle (Fig. 7, B). Furthermore, levels of MMP9 (known to degrade collagen fragments IV and V) were changed (Fig. 7, C), suggesting decreased MMP9 levels in the deltoid compared with the SS muscle.

MMP13 (known to degrade primarily collagen fragments II) mRNA gene expression was absent in SS (0.005 ± 0.006, n = 12) and deltoid (0.002 ± 0.002, n = 16) muscle tissue, whereas MMP13 mRNA gene expression was present in SS tendon tissue (4.95 ± 5.33, n = 4) in RC tear conditions.

A significant negative correlation was found between age of lesion and MMP9 levels ($r = -0.61$, $P = .03$). We found no significant correlation between age of lesion and MMP1 levels ($r = 0.05$, $P = .87$) and a tendency of a correlation with MMP3 levels ($r = -0.46$, $P = .08$).

In line with previous findings in the SS enthesis (reviewed in the paper by Jensen et al[21]), we found that protein levels of MMP1 (known to specifically break down
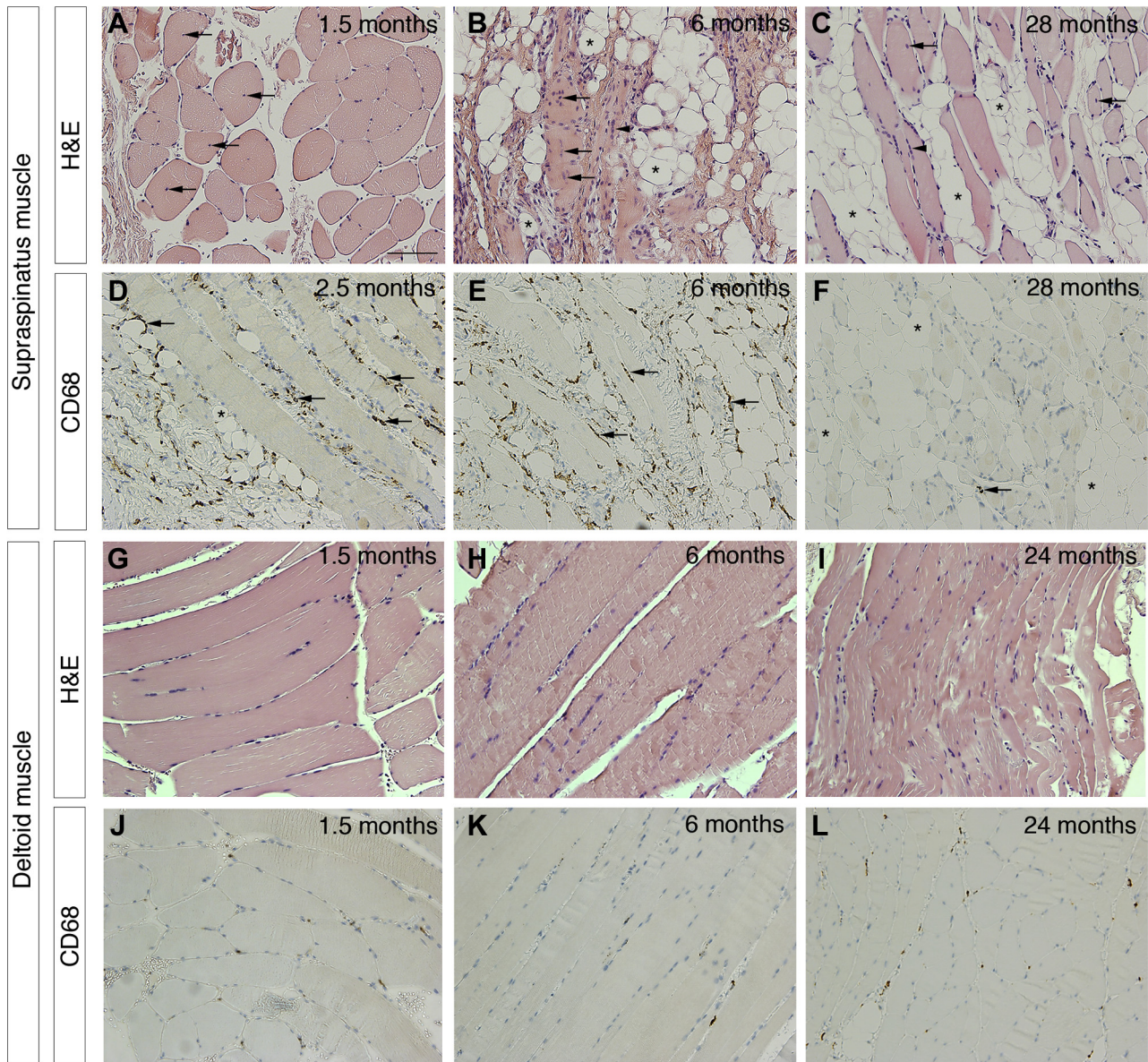
Figure 3 Histologic analysis of the SS muscle. (**A-C**) H&E-stained tissue sections of SS muscle biopsies from representative patients at (**A**) 1½, (**B**) 6, and (**C**) 28 months after the RC tendon tear demonstrating the presence of muscle fibers with internal nuclei (◄—) and nuclear chains (◄). (**D-F**) Immunohistochemical staining of SS muscle biopsies from representative patients at (**D**) 2½, (**E**) 6, and (**F**) 28 months demonstrating the presence of a high number of CD68$^+$ macrophages (◄—) within the first 6 months after the RC tendon tear. Please note the presence of massive fatty cell infiltration (*, asterisks) between muscle fibers already early after the RC tendon tear. (**G-I**) H&E-stained tissue sections of deltoid biopsies from representative patients at (**G**) 1½, (**H**) 6, and (**I**) 24 months after the RC tendon tear. (**J-L**) CD68 immunohistochemical staining of deltoid muscle biopsies from representative patients at (**J**) 1½, (**K**) 6, and (**L**) 24 months after the RC tendon tear. Scale bar: 100 μm. *SS*, supraspinatus; *H&E*, hematoxylin and eosin; *RC*, rotator cuff.

most subtypes of collagen, providing mechanical strength to tissues) were higher in the SS tendon than in muscle tissue (Supplementary Table S8). Also, MMP3 was high in the SS tendon (Supplementary Table S8).

We also investigated changes in TGF, known to be affected in SS enthesis after the RC tear (reviewed in the paper by Jensen et al[21]) (Fig. 7, *D-F*). Levels of TGFβ1 (Fig. 7, *D*) and TGFβ3 (Fig. 7, *F*) were higher in the SS muscle, suggesting increased TGFβ1 and TGFβ3 levels in the SS muscle

compared with the deltoid muscle. We found no correlation between age of lesion and TGFβ1 ($r = 0.12, P = .7$), TGFβ2 ($r = -0.07, P = .83$), or TGFβ3 ($r = -0.32, P = .34$).

Discussion

In this study, we demonstrated massive SS muscle inflammation after the tendon tear combined with fatty infiltration
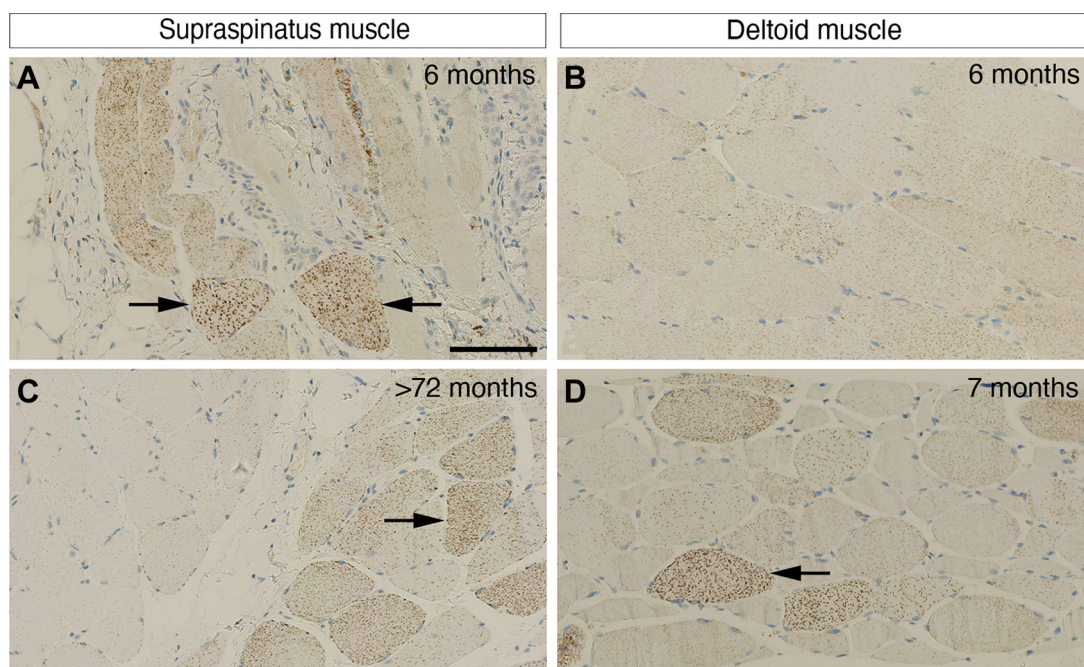
Figure 4 Immunohistochemical staining for adipophilin. (**A**, **B**) Adipophilin expression in (**A**) SS and (**B**) deltoid muscle fibers in a patient with a 6-month-old RC lesion, showing higher adipophilin expression in the SS muscle compared with the deltoid. Adipophilin is seen as a granular staining in the muscle fiber cytoplasm, and because of its localization to the surface of lipid vacuoles, it visualizes the distribution of intracellular lipid. (**C**, **D**) Adipophilin expression in SS and deltoid muscle fibers from (**C**) a patient with a >72-month-old RC tear and (**D**) another patient with a 7-month-old RC lesion. Please note that the distribution of adipophilin can be uneven with different expression in neighboring fascicles in both the SS and deltoid muscles. Scale bar: 100 μm. *RC*, rotator cuff; *SS*, supraspinatus.

and degeneration. Simultaneous changes in the innate immune response, cytokines, and proteins related to extracellular matrix reorganization and mediation of fibrosis in the SS musculature were also seen.

In line with previous experimental studies using mice [27] and rats,[12,15,17] we observed high numbers of infiltrating monocytes/macrophages in the SS muscle in early cases of the tendon tear; this tendency ceased after 24 months, however. Inflammation was (initially) driven by high numbers of infiltrating CD68^{+} macrophages, which are thought to be key sources of TGF-β1 linked to fibrosis in a chronically injured muscle.[29]

Upregulated proteins in the SS muscle compared with the deltoid also showed "neutrophil degranulation" among the most enriched processes. Neutrophils have been identified as the main cells infiltrating the muscle after injury, [45] and neutrophil-derived oxidants extended tissue damage in a rabbit model of stretch skeletal muscle injury.[46] On the other hand, blocking cell infiltration compromised the initial regenerative response, suggesting a role for neutrophils in muscle growth and repair by removal of tissue debris and activation of satellite cells.[46] Moreover, a recent study has shown that neutrophil-secreted proteases can also have an immunoregulatory role by activating IL-33.[9] IL-33 has been shown to be produced by fibro-adipogenic progenitor (FAP) cells, which are uniformly present in the interstitial space in the skeletal muscle and respond to muscle damage.[19] Our observation of higher IL-33 levels in the SS muscle compared with the deltoid muscle indicates an activation of FAPs, which are the source of adipocytes in muscle fatty infiltration. Muscle Foxp3^{+} Tregs are characterized by high levels of expression of the IL-33 receptor, ST2, and are known to potentiate regeneration in acute and chronic injury models.[7] Despite comparable numbers of Foxp3^{+} Tregs/mm^2, we saw a significant decrease in *FOXP3* mRNA levels in the SS muscle compared with the deltoid muscle after the RC tear, suggestive of repressed gene expression in Tregs located in the SS muscle. Many cytokines and factors can negatively regulate *FOXP3* gene expression, including IL-6, IL-7, TGF-β, and G-CSF,[20,31,41] all of which we observed to be different between the SS and deltoid muscle.

The expression of IL-15 has been shown to inhibit fatty infiltration and facilitate muscle regeneration through regulation of FAP cells.[22] In the present study, IL-15 levels were significantly lower in the SS compared with the deltoid muscle, supporting our findings that adipocytes appear in the SS and that the regenerative potential appears to be reduced in the SS muscle after the RC tendon tear.

IL-17 is a proinflammatory cytokine secreted by activated CD4^{+} T-helper cells (Th17), which are highly
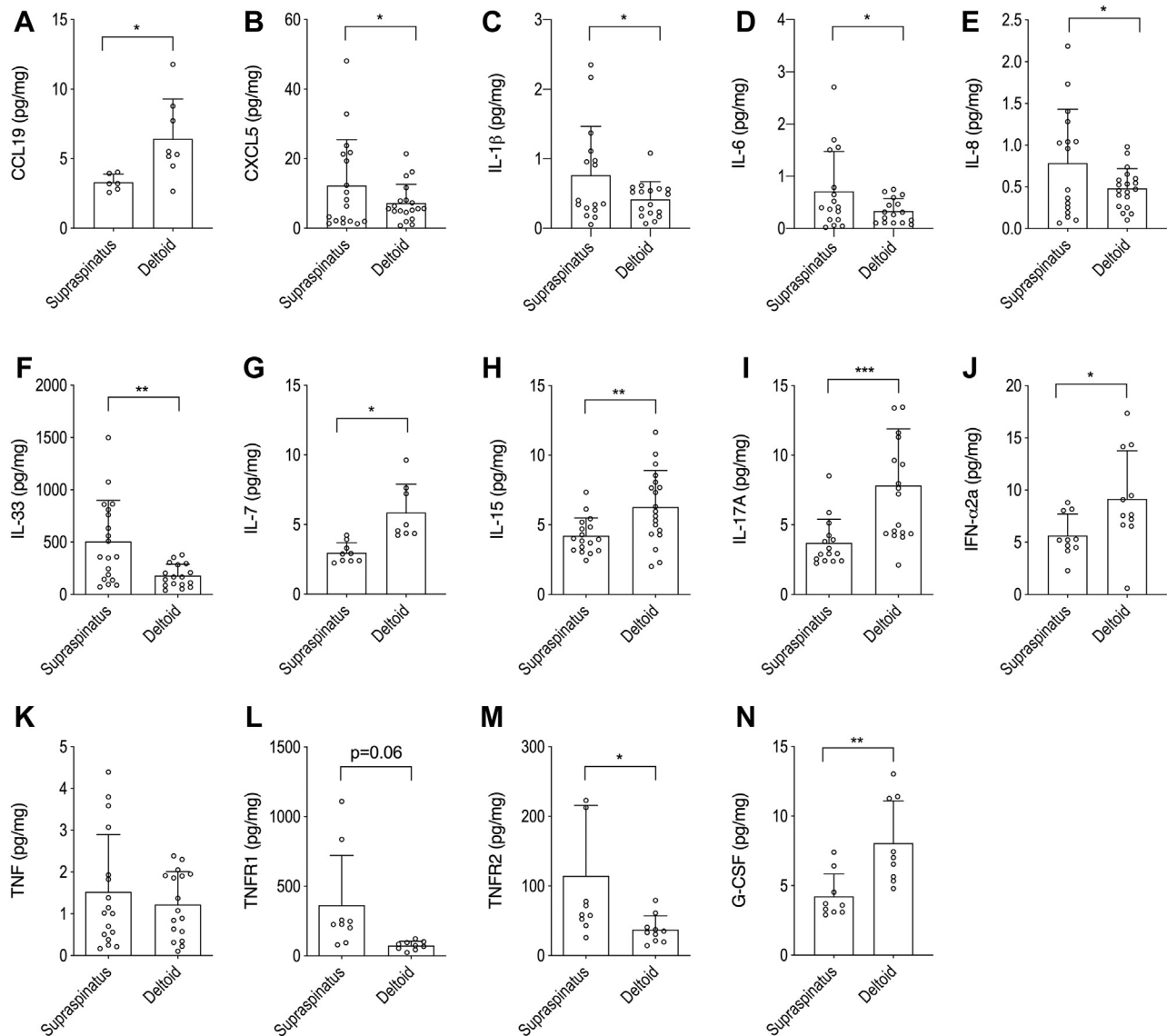
Figure 5 Cytokine and TNF receptor protein expression in SS and deltoid muscle tissue in RC tear conditions. (**A-N**) Electro-chemiluminescence immunoassay analysis of (**A**) CCL19, (**B**) CXCL5, (**C**) IL-1β, (**D**) IL-6, (**E**) IL-8, (**F**) IL-33, (**G**) IL-7, (**H**) IL-15, (**I**) IL-17A, (**J**) INF-α2a, (**K**) TNF, (**L**) TNFR1, (**M**) TNFR2, and (**N**) G-CSF protein levels in SS and deltoid muscle biopsies from patients with an RC tendon tear. $***P < .001$, $**P < .01$. $*P < .05$, Student's t-test (n = 22/group). Samples with CV values above 25% were excluded in individual analyses. *SS*, supraspinatus; *RC*, rotator cuff; *CV*, coefficient of variation.

proinflammatory and induce severe autoimmunity (reviewed in the paper by Kotake et al[26]). IL-17 levels are increased in early human tendinopathy, mediating inflammatory and tissue remodeling events,[33] and IL-17 inhibits myoblast differentiation.[25] In the present study, IL-17 levels were significantly lower in the SS than in the deltoid muscle, but the exact relevance of decreased IL-17 levels remains to be elucidated.

Our GO analysis showed changes in "extracellular matrix organization" and "degradation of extracellular matrix" especially due to the upregulation of CMA1, COL5A3, CTSS, ELN, and MMP19 in the SS compared

with the deltoid muscle. To our knowledge, no one has investigated MMP levels in the human SS muscle under tear conditions. MMPs are a large group or proteolytic enzymes responsible for tissue remodeling and degradation of the extracellular matrix. In our study, MMP3 and MMP9 levels were significantly increased in the SS compared with the deltoid muscle. MMP3 is one of the primary activators of MMP9 from its inactive proenzyme form.[35] MMP9 is produced by a variety of cells, including fibroblasts. MMP9 appears to be a regulatory factor in neutrophil migration across the basement membrane,[47] and it also performs several important

Table I Cytokine analysis in patients with a RC tear

	SS muscle (pg/mg)	Deltoid muscle (pg/mg)	P value
IL-1α	2.44 ± 1.38 (n = 13)	2.21 ± 1.72 (n = 15)	.83
IL-1Ra	46.83 ± 20.24 (n = 14)	34.40 ± 12.94 (n = 15)	.33
IL-2	0.64 ± 0.47 (n = 4)	0.41 ± 0.24 (n = 5)	.50
IL-2Ra	93.08 ± 56.28 (n = 8)	99.11 ± 76.81 (n = 7)	.87
IL-4	0.04 ± 0.07 (n = 6)	0.07 ± 0.08 (n = 6)	.53
IL-9	1.12 ± 0.72 (n = 16)	1.10 ± 0.62 (n = 17)	.98
IL-12/IL-23p40	14.35 ± 29.01 (n = 15)	14.64 ± 7.71 (n = 18)	.78
IL-12p70	0.23 ± 0.07 (n = 6)	0.39 ± 0.32 (n = 7)	.55
IL-13	2.76 ± 2.25 (n = 3)	4.35 ± 3.68 (n = 3)	.31
MIF	28,656 ± 18,419 (n = 9)	26,617 ± 19,295 (n = 8)	.36
IFN-β	46.08 ± 27.05 (n = 8)	34.05 ± 37.80 (n = 7)	.56
IFN-γ	2.23 ± 3.48 (n = 5)	2.92 ± 2.11 (n = 4)	.95
FLT3L	14.29 ± 5.13 (n = 5)	15.01 ± 8.78 (n = 4)	.93
TRAIL	54.41 ± 23.81 (n = 17)	47.00 ± 17.70 (n = 19)	.50
CXCL1/GROα	2.63 ± 2.05 (n = 9)	3.92 ± 3.37 (n = 8)	.16
CXCL10/IP-10	8.73 ± 4.00 (n = 7)	8.69 ± 2.94 (n = 9)	.86
CXCL11/I-TAC	6.74 ± 2.02 (n = 15)	7.78 ± 3.00 (n = 19)	.28
CCL2/MCP1	4.03 ± 2.38 (n = 8)	4.83 ± 2.17 (n = 9)	.33
CCL3/MIP-1α	4.58 ± 2.35 (n = 5)	4.01 ± 4.05 (n = 2)	–
CCL4/MIP-1β	5.17 ± 1.62 (n = 9)	6.35 ± 1.54 (n = 8)	.29
CCL7/MCP-3	4.92 ± 2.59 (n = 8)	4.03 ± 3.41 (n = 6)	.33
CCL8/MCP-2	1.52 ± 0.76 (n = 8)	1.71 ± 1.11 (n = 4)	.48
CCL13/MCP4	15.64 ± 11.80 (n = 8)	9.57 ± 7.33 (n = 7)	.24
CCL17/TARC	3.05 ± 1.01 (n = 7)	3.40 ± 0.59 (n = 8)	.41
M-CSF	5.45 ± 3.46 (n = 9)	6.27 ± 3.39 (n = 6)	.84
GM-CSF	0.13 ± 0.14 (n = 3)	0.10 ± 0.11 (n = 7)	.33
LT-α	1.60 ± 0.79 (n = 6)	1.67 ± 0.61 (n = 9)	.41
YKL-40/CHI3L1	121.40 ± 37.64 (n = 5)	340.80 ± 274.40 (n = 9)	.18
VEGF-A	93.36 ± 31.19 (n = 7)	134.40 ± 53.22 (n = 9)	.19

RC, rotator cuff; *SS*, supraspinatus.
Paired Student's *t*-test.

functions within neutrophil action[26] such as degrading the extracellular matrix, activation of IL-1β, and cleavage of several chemokines.[36] In vitro studies have demonstrated that inhibition of MMP9 reduced the levels of active TGF-β1 and reduced several TGF-β1-driven responses such as fibroblast stimulation.[24] In this context, MMP9 appears to activate or stimulate the release of a number of cytokines and growth factors, including TGF-β1,[30] which we found to be elevated in the SS compared with the deltoid muscle. MMP9 activity positively correlated with skeletal muscle atrophy in immobilized rats,[40] supporting a role in muscle atrophy. This is in line with our present findings of a positive correlation between MMP9 levels and age of an RC lesion. Altogether, this suggests that MMP9 plays an important role in SS muscle remodeling.

Although only a few studies have applied a large-scale proteomics approach to address RC pathophysiology, these studies combined found several markers indicative of tissue remodeling and suggested an untapped potential for proteomics in tendon research (reviewed in the paper by Sejersen et al[42]). A multiomics methodology applied to a rat RC injury model to study myosteatosis identified disrupted mitochondrial function as one of the underlying mechanisms of lipid accumulation in muscle fibers.[18] In our study, we identified 32 downregulated mitochondrial proteins, 15 of which are associated with mitochondrial electron transport chain. Mitochondrial dysfunction reduces energy production, and the dysfunction of these organelles has been connected to the myosteatosis that is commonly reported after RC tendon injury.[3] Our finding of steatotic adipophilin positive muscle fibers and changes in lipid metabolism and mitochondrial function supports this connection.

This study has certain inherent limitations related to the variability of disease severity and duration and the sample size, and the results are biased toward patients with RC tears who chose to undergo surgery. The enrolled patients
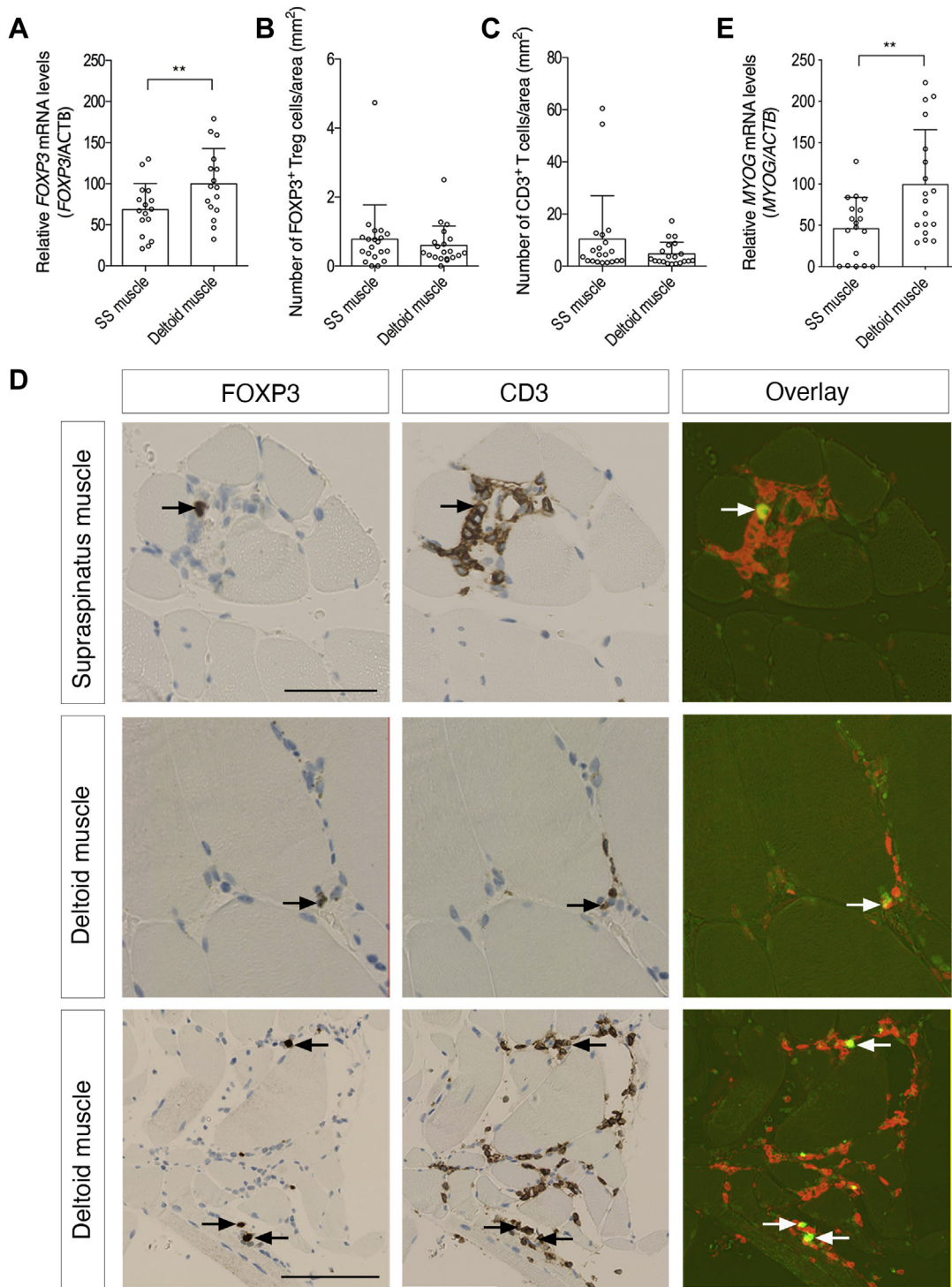
Figure 6 *FOXP3* and *MYOG* mRNA expression is lower in SS muscle than in deltoid muscle tissue in RC tear conditions. (**A**) *FOXP3* mRNA levels in SS and deltoid muscle biopsies demonstrated significantly lower expression levels in the SS compared with the deltoid muscle. $**P < .01$, paired Student's *t*-test (n = 18/group). Two outliers in the SS muscle and 2 outliers in the deltoid muscle group were removed according to ROUT's outlier test. (**B**) The number of FOXP3^{+} Tregs/mm^2 and (**C**) the total number of CD3^{+} T cells were comparable between the SS and deltoid muscle in RC tear conditions. (**D**) Representative FOXP3 and CD3 immunohistochemically stained tissue sections from SS and deltoid muscle demonstrating overlay between subsets of FOXP3^{+} and CD3^{+} T cells, representing the presence of Tregs (arrows) in both SS and deltoid muscle in RC tear conditions. Scale bars: 50 μm (top and middle panels) and 100 μm (bottom panel). (**E**) *MYOG* mRNA levels in SS and deltoid muscle biopsies demonstrated significantly lower expression levels in the SS compared with the deltoid muscle. $**P < .01$, paired Student's t-test (n = 18/group). *SS*, supraspinatus; *RC*, rotator cuff.
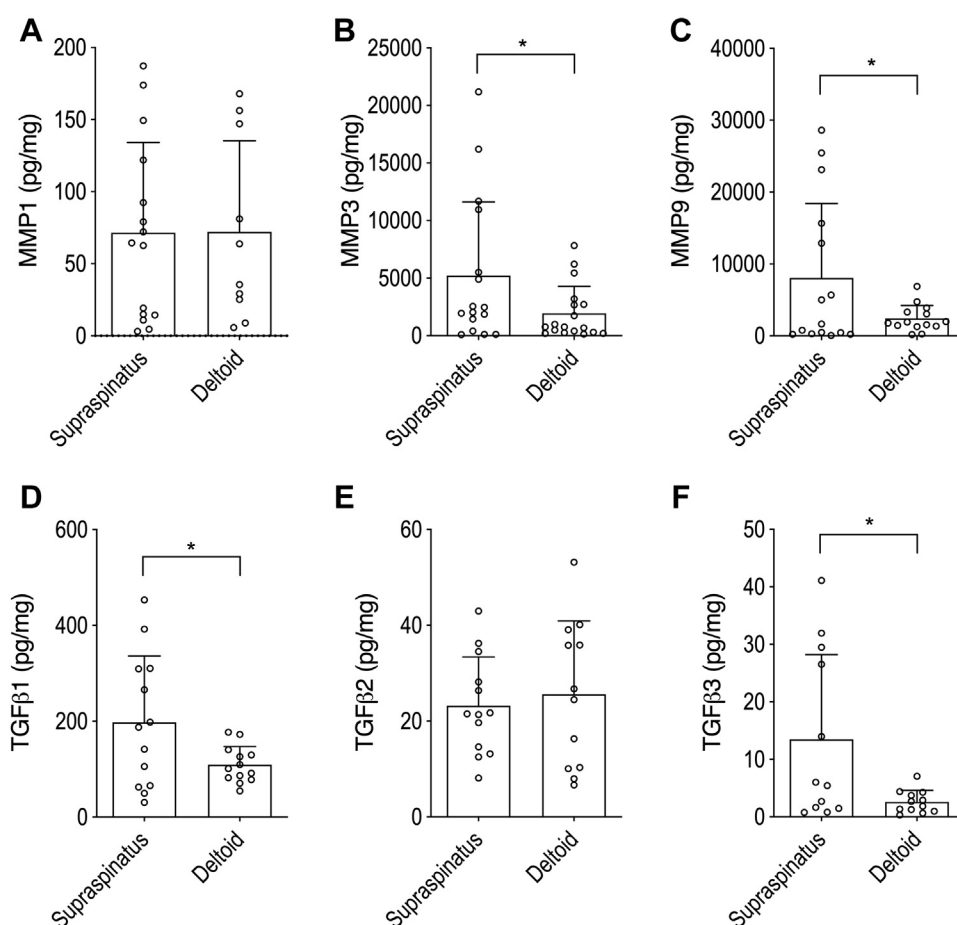
Figure 7 Matrix metalloprotease and transforming growth factor-β protein expression in SS and deltoid muscle tissue under RC tear conditions. (A-F) Electrochemiluminescence immunoassay analysis of (A) MMP1, (B) MMP3, (C) MMP9, (D) TGFβ1, (E) TGFβ2, and (F) TGFβ3 protein levels in SS and deltoid muscle biopsies from patients with an RC tendon tear. *$P < .05$, Student's test (n = 22/group). Samples with CV values above 25% were excluded in individual analyses. *SS*, supraspinatus; *RC*, rotator cuff.

comprised 4 smokers and 7 patients who received pain killers on a daily basis. The adverse consequences of smoking and mild anti-inflammatory drug intake on the inflammatory response were not assessed because of lack of statistical power. Another limitation inherent in muscle biopsy studies is the difficulty of ensuring uniform biopsy procedures, which are important to secure reproducibility and to account for regional variations in protein composition. In this study, biopsies were obtained close to the musculotendinous junction of the SS muscle in all patients using an all-arthroscopic approach from the bursal side, limiting possible location-dependent variations.

The rationale for using the deltoid muscle for comparison could be challenged as it may be asymptomatically affected. The ipsilateral deltoid has been used as a standard of reference in a number of studies,[2,47] also justifying the use of paired statistics and increasing the power of the analyses.

Conclusions

This study demonstrated massive muscle changes after the SS tendon tear characterized by high numbers of inflammatory macrophages in lesions less than 3 months old and overall changes in cytokine levels, MMP levels, and growth factors. Our proteome analysis demonstrated that proteins involved in inflammation, extracellular matrix reorganization, and lipid metabolism were among the most enriched. Knowing that massive inflammation with infiltration of immune cells into the RC musculotendinous lesion disrupts normal muscle regeneration, this implies that intervention with the repair of the tendon lesion and concomitant target-specific adjuvant treatment of the inflammatory state of the SS muscle could be key to improving RC muscle recovery.

Supplementary Data

Supplementary data to this article can be found online at https://doi.org/10.1016/j.jse.2020.08.028.

References

1. Abrams GD, Luria A, Carr RA, Rhodes C, Robinson WH, Sokolove J. Association of synovial inflammation and inflammatory mediators with glenohumeral rotator cuff pathology. J Shoulder Elbow Surg 2016;25:989-97. https://doi.org/10.1016/j.jse.2015.10.011
2. Ashry R, Schweitzer ME, Cunningham P, Cohen J, Babb J, Cantos A. Muscle atrophy as a consequence of rotator cuff tears: should we compare the muscles of the rotator cuff with those of the deltoid? Skeletal Radiol 2007;36:841-5. https://doi.org/10.1007/s00256-007-0307-5
3. Bedi A, Dines J, Warren RF, Dines DM. Massive tears of the rotator cuff. J Bone Joint Surg Am 2010;92:1894-908. https://doi.org/10.2106/JBJS.I.01531
4. Bennike TB, Carlsen TG, Ellingsen T, Bonderup OK, Glerup H, Bogsted M, et al. Neutrophil extracellular traps in ulcerative colitis: a proteome analysis of intestinal biopsies. Inflamm Bowel Dis 2015;21:2052-67. https://doi.org/10.1097/MIB.0000000000000460
5. Benson RT, McDonnell SM, Knowles HJ, Rees JL, Carr AJ, Hulley PA. Tendinopathy and tears of the rotator cuff are associated with hypoxia and apoptosis. J Bone Joint Surg Br 2010;92:448-53. https://doi.org/10.1302/0301-620X.92B3.23074
6. Blaine TA, Kim YS, Voloshin I, Chen D, Murakami K, Chang SS, et al. The molecular pathophysiology of subacromial bursitis in rotator cuff disease. J Shoulder Elbow Surg 2005;14:84S-9S. https://doi.org/10.1016/j.jse.2004.09.022
7. Burzyn D, Kuswanto W, Kolodin D, Shadrach JL, Cerletti M, Jang Y, et al. A special population of regulatory T cells potentiates muscle repair. Cell 2013;155:1282-95. https://doi.org/10.1016/j.cell.2013.10.054
8. Chen J, Bardes EE, Aronow BJ, Jegga AG. ToppGene Suite for gene list enrichment analysis and candidate gene prioritization. Nucleic Acids Res 2009;37:W305-11. https://doi.org/10.1093/nar/gkp427
9. Clancy DM, Sullivan GP, Moran HBT, Henry CM, Reeves EP, McElvaney NG, et al. Extracellular neutrophil proteases are efficient regulators of IL-1, IL-33, and IL-36 cytokine activity but poor effectors of microbial killing. Cell Rep 2018;22:2937-50. https://doi.org/10.1016/j.celrep.2018.02.062
10. Cofield RH, Parvizi J, Hoffmeyer PJ, Lanzer WL, Ilstrup DM, Rowland CM. Surgical repair of chronic rotator cuff tears. A prospective long-term study. J Bone Joint Surg Am 2001;83:71-7.
11. Cua DJ, Tato CM. Innate IL-17-producing cells: the sentinels of the immune system. Nat Rev Immunol 2010;10:479-89. https://doi.org/10.1038/nri2800
12. Davies MR, Lee L, Feeley BT, Kim HT, Liu X. Lysophosphatidic acid-induced RhoA signaling and prolonged macrophage infiltration worsens fibrosis and fatty infiltration following rotator cuff tears. J Orthop Res 2017;35:1539-47. https://doi.org/10.1002/jor.23384
13. Gibbons MC, Singh A, Anakwenze O, Cheng T, Pomerantz M, Schenk S, et al. Histological evidence of muscle degeneration in advanced human rotator cuff disease. J Bone Joint Surg Am 2017;99:190-9. https://doi.org/10.2106/JBJS.16.00335
14. Gladstone JN, Bishop JY, Lo IK, Flatow EL. Fatty infiltration and atrophy of the rotator cuff do not improve after rotator cuff repair and correlate with poor functional outcome. Am J Sports Med 2007;35:719-28. https://doi.org/10.1177/0363546506297539
15. Gumucio JP, Davis ME, Bradley JR, Stafford PL, Schiffman CJ, Lynch EB, et al. Rotator cuff tear reduces muscle fiber specific force production and induces macrophage accumulation and autophagy. J Orthop Res 2012;30:1963-70. https://doi.org/10.1002/jor.22168
16. Gumucio J, Flood M, Harning J, Phan A, Roche S, Lynch E, et al. T lymphocytes are not required for the development of fatty degeneration after rotator cuff tear. Bone Joint Res 2014;3:262-72. https://doi.org/10.1302/2046-3758.39.2000294
17. Gumucio JP, Korn MA, Saripalli AL, Flood MD, Phan AC, Roche SM, et al. Aging-associated exacerbation in fatty degeneration and infiltration after rotator cuff tear. J Shoulder Elbow Surg 2014;23:99-108. https://doi.org/10.1016/j.jse.2013.04.011
18. Gumucio JP, Qasawa AH, Ferrara PJ, Malik AN, Funai K, McDonagh B, et al. Reduced mitochondrial lipid oxidation leads to fat accumulation in myosteatosis. FASEB J 2019;33:7863-81. https://doi.org/10.1096/fj.201802457RR
19. Hejbol EK, Hajjaj MA, Nielsen O, Schroder HD. Marker expression of interstitial cells in human skeletal muscle: an immunohistochemical study. J Histochem Cytochem 2019;67:825-44. https://doi.org/10.1369/0022155419871033
20. Heninger AK, Theil A, Wilhelm C, Petzold C, Huebel N, Kretschmer K, et al. IL-7 abrogates suppressive activity of human CD4+CD25+FOXP3+ regulatory T cells and allows expansion of alloreactive and autoreactive T cells. J Immunol 2012;189:5649-58. https://doi.org/10.4049/jimmunol.1201286
21. Jensen PT, Lambertsen KL, Frich LH. Assembly, maturation, and degradation of the supraspinatus enthesis. J Shoulder Elbow Surg 2018;27:739-50. https://doi.org/10.1016/j.jse.2017.10.030
22. Kang X, Yang MY, Shi YX, Xie MM, Zhu M, Zheng XL, et al. Interleukin-15 facilitates muscle regeneration through modulation of fibro/adipogenic progenitors. Cell Commun Signal 2018;16:42. https://doi.org/10.1186/s12964-018-0251-0
23. Karjalainen TV, Jain NB, Heikkinen J, Johnston RV, Page CM, Buchbinder R. Surgery for rotator cuff tears. Cochrane Database Syst Rev 2019;12:CD013502. https://doi.org/10.1002/14651858.CD013502
24. Kobayashi T, Kim H, Liu X, Sugiura H, Kohyama T, Fang Q, et al. Matrix metalloproteinase-9 activates TGF-beta and stimulates fibroblast contraction of collagen gels. Am J Physiol Lung Cell Mol Physiol 2014;306:L1006-15. https://doi.org/10.1152/ajplung.00015.2014

25. Kocic J, Santibanez JF, Krstic A, Mojsilovic S, Ilic V, Bugarski D. Interleukin-17 modulates myoblast cell migration by inhibiting urokinase type plasminogen activator expression through p38 mitogen-activated protein kinase. Int J Biochem Cell Biol 2013;45:464-75. https://doi.org/10.1016/j.biocel.2012.11.010

26. Kotake S, Yago T, Kawamoto M, Nanke Y. Role of osteoclasts and interleukin-17 in the pathogenesis of rheumatoid arthritis: crucial 'human osteoclastology'. J Bone Miner Metab 2012;30:125-35. https://doi.org/10.1007/s00774-011-0321-5

27. Krieger JR, Tellier LE, Ollukaren MT, Temenoff JS, Botchwey EA. Quantitative analysis of immune cell subset infiltration of supraspinatus muscle after severe rotator cuff injury. Regen Eng Transl Med 2017;3:82-93. https://doi.org/10.1007/s40883-017-0030-2

28. Kuenzler MB, Nuss K, Karol A, Schar MO, Hottiger M, Raniga S, et al. Neer Award 2016: reduced muscle degeneration and decreased fatty infiltration after rotator cuff tear in a poly(ADP-ribose) polymerase 1 (PARP-1) knock-out mouse model. J Shoulder Elbow Surg 2017;26:733-44. https://doi.org/10.1016/j.jse.2016.11.009

29. Liu X, Joshi SK, Ravishankar B, Laron D, Kim HT, Feeley BT. Upregulation of transforming growth factor-beta signaling in a rat model of rotator cuff tears. J Shoulder Elbow Surg 2014;23:1709-16. https://doi.org/10.1016/j.jse.2014.02.029

30. Longo GM, Xiong W, Greiner TC, Zhao Y, Fiotti N, Baxter BT. Matrix metalloproteinases 2 and 9 work in concert to produce aortic aneurysms. J Clin Invest 2002;110:625-32. https://doi.org/10.1172/JCI15334

31. Maruyama T, Konkel JE, Zamarron BF, Chen W. The molecular mechanisms of Foxp3 gene regulation. Semin Immunol 2011;23:418-23. https://doi.org/10.1016/j.smim.2011.06.005

32. Matthews TJ, Hand GC, Rees JL, Athanasou NA, Carr AJ. Pathology of the torn rotator cuff tendon. Reduction in potential for repair as tear size increases. J Bone Joint Surg Br 2006;88:489-95. https://doi.org/10.1302/0301-620X.88B4.16845

33. Millar NL, Akbar M, Campbell AL, Reilly JH, Kerr SC, McLean M, et al. IL-17A mediates inflammatory and tissue remodelling events in early human tendinopathy. Sci Rep 2016;6:27149. https://doi.org/10.1038/srep27149

34. Navarro P, Trevisan-Herraz M, Bonzon-Kulichenko E, Nunez E, Martinez-Acedo P, Perez-Hernandez D, et al. General statistical framework for quantitative proteomics by stable isotope labeling. J Proteome Res 2014;13:1234-47. https://doi.org/10.1021/pr4006958

35. Ogata Y, Enghild JJ, Nagase H. Matrix metalloproteinase 3 (stromelysin) activates the precursor for the human matrix metalloproteinase 9. J Biol Chem 1992;267:3581-4.

36. Opdenakker G, Van den Steen PE, Dubois B, Nelissen I, Van Coillie E, Masure S, et al. Gelatinase B functions as regulator and effector in leukocyte biology. J Leukoc Biol 2001;69:851-9.

37. Pasternak B, Aspenberg P. Metalloproteinases and their inhibitors-diagnostic and therapeutic opportunities in orthopedics. Acta Orthop 2009;80:693-703. https://doi.org/10.3109/17453670903448257

38. Perez-Riverol Y, Csordas A, Bai J, Bernal-Llinares M, Hewapathirana S, Kundu DJ, et al. The PRIDE database and related tools and resources in 2019: improving support for quantification data. Nucleic Acids Res 2019;47:D442-50. https://doi.org/10.1093/nar/gky1106

39. Petersson SJ, Christensen LL, Kristensen JM, Kruse R, Andersen M, Hojlund K. Effect of testosterone on markers of mitochondrial oxidative phosphorylation and lipid metabolism in muscle of aging men with subnormal bioavailable testosterone. Eur J Endocrinol 2014;171:77-88. https://doi.org/10.1530/EJE-14-0006

40. Reznick AZ, Menashe O, Bar-Shai M, Coleman R, Carmeli E. Expression of matrix metalloproteinases, inhibitor, and acid phosphatase in muscles of immobilized hindlimbs of rats. Muscle Nerve 2003;27:51-9. https://doi.org/10.1002/mus.10277

41. Rutella S, Pierelli L, Bonanno G, Sica S, Ameglio F, Capoluongo E, et al. Role for granulocyte colony-stimulating factor in the generation of human T regulatory type 1 cells. Blood 2002;100:2562-71. https://doi.org/10.1182/blood-2001-12-0291

42. Sejersen MH, Frost P, Hansen TB, Deutch SR, Svendsen SW. Proteomics perspectives in rotator cuff research: a systematic review of gene expression and protein composition in human tendinopathy. PLoS One 2015;10:e0119974. https://doi.org/10.1371/journal.pone.0119974

43. Shannon P, Markiel A, Ozier O, Baliga NS, Wang JT, Ramage D, et al. Cytoscape: a software environment for integrated models of biomolecular interaction networks. Genome Res 2003;13:2498-504. https://doi.org/10.1101/gr.1239303

44. Shindle MK, Chen CC, Robertson C, DiTullio AE, Paulus MC, Clinton CM, et al. Full-thickness supraspinatus tears are associated with more synovial inflammation and tissue degeneration than partial-thickness tears. J Shoulder Elbow Surg 2011;20:917-27. https://doi.org/10.1016/j.jse.2011.02.015

45. St Pierre Schneider B, Brickson S, Corr DT, Best T. CD11b+ neutrophils predominate over RAM11+ macrophages in stretch-injured muscle. Muscle Nerve 2002;25:837-44. https://doi.org/10.1002/mus.10109

46. Toumi H, F'Guyer S, Best TM. The role of neutrophils in injury and repair following muscle stretch. J Anat 2006;208:459-70. https://doi.org/10.1111/j.1469-7580.2006.00543.x

47. de Witte PB, Werner S, ter Braak LM, Veeger HE, Nelissen RG, de Groot JH. The supraspinatus and the deltoid—not just two arm elevators. Hum Mov Sci 2014;33:273-83. https://doi.org/10.1016/j.humov.2013.08.010

48. Yamaguchi K, Ditsios K, Middleton WD, Hildebolt CF, Galatz LM, Teefey SA. The demographic and morphological features of rotator cuff disease. A comparison of asymptomatic and symptomatic shoulders. J Bone Joint Surg Am 2006;88:1699-704. https://doi.org/10.2106/JBJS.E.00835

49. Zhao L, Qiu DK, Ma X. Th17 cells: the emerging reciprocal partner of regulatory T cells in the liver. J Dig Dis 2010;11:126-33. https://doi.org/10.1111/j.1751-2980.2010.00428.x